An Advanced Immersion Level Prediction Using Ensemble Classifier with Heuristic Search Algorithm in 3D Games Content Generated Virtual Environments

Kamalanathan Sundararajan[1], Prasanna Santhanam[2,*]

[1]Assistant Professor Grade-1, VIT School of Design, Vellore Institute of Technology, Vellore, 632014, India

[2]Professor Grade-1, School of Computer Science Engineering and Information Systems , Vellore Institute of Technology, Vellore, 632014, India

Emails: kamalanathan.s@vit.ac.in; sprasanna@vit.ac.in

Abstract

Nowadays, virtual reality (VR) and immersive environments are research fields used in various educational and scientific areas. Immersive digital media desires new techniques for its immersive and interactive features it implies the model of new relationships and narratives with users. VR and technologies related to the virtuality sequence, like digital and immersive environments, are developing media. 3D environments generated with VR compatibility can be skilled from a stereoscopic and egocentric view that outperforms the immersion of the 'classical' screen-based view of 3D gamed virtual environments. Recent video games have complete, interactive scenes generated with innovative modeling and animation software and provided with hardware speeded-up graphics and physics. Their communication takes place with body-based sensing and commodity 3D motion controllers, like and in certain ways more progressive, than those discovered in conventional VEs do. Currently, artificial intelligence-based deep learning (DL) methods have been progressively applied to identify and assess user immersion levels in VR environments. In this paper, we present an Advanced Immersion Level Prediction Using Ensemble Classification Model and Metaheuristic Optimization Algorithm (ILPECM-MOA) in 3D Games Virtual Environments. This paper aims to develop a predictive model for assessing advanced immersion levels in 3D game virtual environments using behavioral and contextual data. At the primary stage, the data pre-processing stage uses Z-score normalization to transform input data into a beneficial pattern. Followed by, the presented ILPECM-MOA method designs ensemble models such as the temporal convolutional network (TCN) model, sparse denoising autoencoder (SDAE) method, and stacked long short-term memory (SLSTM) technique for the classification process. At last, the Hybrid ebola and Bald Eagle search optimization (HEBEO) approach fine-tunes the hyperparameter values of ensemble methods and results in the superior performance of classification. The effectiveness of the ILPECM-MOA model has been validated by the detailed studies utilizing the benchmark dataset. The mathematical outcome indicates that the ILPECM-MOA approach has improved performance and scalability in terms of various measures over the recent methods.

Keywords: Immersion Level Prediction; 3D Games; Virtual Environments; Ensemble Classification Model; Metaheuristic Optimization Algorithm

1. Introduction

Immersive and communicating technologies like Virtual Reality (VR) are a novel breakthrough in how people are in touch with the environment and perceive novel methods in these relationships with reality [1]. VR and other immersive Information and Communication Technologies (ICT) have a higher ability to transform the real world and how we interact with it. Therefore, as VR is an effective tool for bringing transformations in social reality, it is essential to determine and examine its possible consequences and impact on what means new media and communication technologies can produce new messages and cultural techniques [2]. Immersive technology and

DOI: https://doi.org/10.54216/FPA.210120
Received: March 16, 2025 Revised: June 06, 2025 Accepted: July 16, 2025

VR have transformed the experience and interaction of people with augmented reality (AR) environments. VR comprises a simulated three-dimensional (3D) setting formed through computers that users can interact with and navigate [3]. VR is usually experienced using a VR headset, which frequently immerses the users, along with other sensory inputs, like sound and touch.

In contrast, Immersive technology comprises a wide array of tools that intend to completely involve the senses of the user and make an extremely immersive encounter [4]. This contains VR, mixed reality (MR), AR, and other interrelated technologies. This immersive technology has established applications in several domains, such as entertainment, gaming, training, education, and healthcare, contributing interesting opportunities to create engaging and realistic experiences that were once limited only to our thoughts [5]. Video gameplay and rich game environments are deeply dissimilar from standard virtual environments (VEs), in which the novel rules for 3D selection were formed. Present video games have thorough, cooperative scenes formed with animation software and sophisticated modelling and are favoured with hardware-accelerated physics and graphics [6]. Their interaction happens with body-based sensing and commodity 3D motion controllers and is somewhat more innovative than those in conventional VEs are. Intrinsically, rules for 3D selection are less significant in those game-based VEs that normally have dynamic moving and thickly packed objects in the landscape, for both reality and gameplay parts [7].

VR integrates 3D technologies that provide a realistic illusion. VR produces a simulation of real-life circumstances. Consequently, VR denotes a viewer-cantered, 3D computer-generated environment, multi-sensory, interactive, and immersive the incorporation of tools required for creating such an environment [8]. VR technology acts out natural stereoscopic viewing procedures through computer technology for creating left-eye and right-eye images of a provided 3D object or scene. The viewer's brain incorporates the information from these dual viewpoints to build the 3D space perception. Therefore, VR technology produces the illusion that the on-screen object has profundity and existence away from the flat image projected on the screen [9]. By VR, viewers observe distance and spatial relations among diverse object modules precisely and practically when compared with traditional visualization tools. Artificial intelligence (AI) methods are gradually used to identify and measure user immersion extents in VR environments. Through deep learning (DL) models, scholars wanted to detect and analyse numerous user physiological and behavioural signals to estimate the immersion level encountered by people in the VR environment [10].

In this paper, we present an Advanced Immersion Level Prediction Using Ensemble Classification Model and Metaheuristic Optimization Algorithm (ILPECM-MOA) in 3D Games Virtual Environments. At first, the data pre-processing stage uses Z-score normalization. Next, the presented ILPECM-MOA method designs ensemble models such as the temporal convolutional network (TCN) model, sparse denoising autoencoder (SDAE) method, and stacked long short-term memory (SLSTM) technique for the classification process. Finally, the Hybrid ebola and bald eagle search optimization (HEBEO) approach fine-tunes the hyperparameter values of ensemble methods and results in the superior performance of classification. The mathematical outcome indicates that the ILPECM-MOA approach has improved performance and scalability in terms of various measures over the recent methods.

2. Prior Research on 3D Games Virtual Environments

Lee et al. [11] proposed a new system to efficiently estimate partial lower and upper body actions in a VR environment utilizing merely head movements and the corresponding head rotation axis, without needing other hardware. This system computes the angle between the head rotation axis and the pelvis of the avatar for naturally reproducing the lower body bending and upper body inclination of the user. Particularly, it provides the benefit of effectively employing inadequate computational resources in multiplayer environments. Gursesli et al. [12] focused on the VR and AR dynamics. It gives an overview of historical growth and the deep effect of those techniques, offering a full understanding of their role in HCI. This section provides a vision of the VR and AR progression, from theoretical development to real-world use with HCI. Xu et al. [13] presented a wireless multiuser interactive VR alongside an edge-device collective calculating architecture to rectify the motion-to-photon (MTP) threshold bottleneck. The rendering background tiles indices in the forecast window are defined and the selected background and foreground tiles are stacked into the relevant handling queues depending on the location of the rendering.

Lyu and Wang [14] introduced a model for immersive 3D visualization of sub-surface ground architypes in geo-applications leveraging VR. At first, the 3D sub-surface archetype was designed from restricted borehole data in a data-driven way. Afterward, a VR scheme is created by relevant hardware and software devices presently existing in markets for immersive visualization as well as communication with the created 3D sub-surface ground architecture. Ojha et al. [15] presented a different and stimulating concept named VR horror sports, combining horror factors with sports in the VR platform. A unique method for emerging adaptive VR horror games by merging player-modelling methodologies alongside an adaptive means-enabled model, which learns players' fear and consequently alters the content of the game. This research offers two important advances: a new approach to

DOI: https://doi.org/10.54216/FPA.210120
Received: March 16, 2025 Revised: June 06, 2025 Accepted: July 16, 2025

determine a player's fears through ML and game data, and an adaptive game system, which uses an agent to observe players' fears and limit contact to factors they find distressing. Kumar et al. [16] focused on the 3D gamification effects through the AI-incorporated Internet of Medical Things (AIoMT) applied with a VR for medical and biology students for learning the brain of humans. Currently, practical and theoretical learning integrates AR and VR. This research concentrated on using 3D animation, VR, and simulation in medical education.

Yamazaki and Hasegawa [17] intended to increase the VR shooting games experience by deploying a 3D haptic direction technique utilizing belt- and necklace-type haptic devices. This device assists in modulating the vibrations produced and coordinates with musical signals as per the azimuth and target heights within 3D space that can be anticipated to advance the gaming experience. Agarwal and Shridevi [18] addressed the necessity for efficient disaster evacuation training approaches by presenting a VR method that employs Reinforcement Learning Procedural Content Generation (RL-PCG) frameworks. This work aims to give an inexpensive and secure way for conducting disaster evacuation preparedness training, exceeding the restrictions of classical drills. The goal is to incorporate a 3-layer PCG design to generate realistic VR disaster simulations.

3. Algorithm and System Design

In this paper, we present an Advanced ILPECM-MOA in 3D Games Virtual Environments. This paper aims to develop a predictive model for assessing advanced immersion levels in 3D game virtual environments using behavioral and contextual data. It comprises data preprocessing, ensemble classification, and parameter tuning models. Fig. 1 exemplifies the entire workflow of the ILPECM-MOA method.

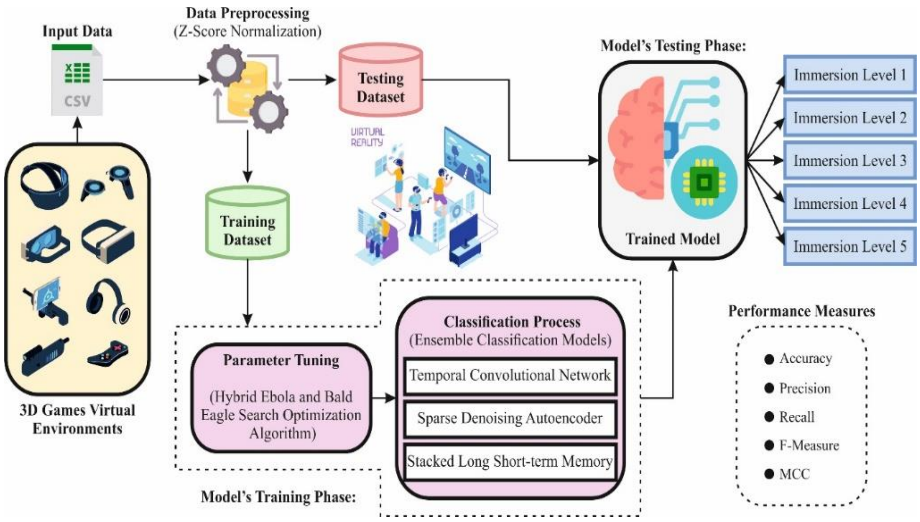

Figure 1. Entire Workflow of ILPECM-MOA Method

A. Data Pre-processing using Z-score

At the primary stage, the data pre-processing stage uses Z-score normalization to transform input data into a beneficial pattern. Z-score normalization is a statistical model employed to handle the process of data outliers and standardizing attributes [19]. It creates the feature values utilizing standard deviation and means, thus safeguarding comparability through variables. This z-score normalization further enhances the efficacy. The transformation is carried out utilizing the succeeding Eq. (1).

$$u' = \frac{u - \mu}{\sigma} \tag{1}$$

Here μ represents the mean value of features and σ signifies the determined feature's standard deviation. Values are equal to the mean mapped to zero while the Z-score normalization model has been implemented; values are greater or lesser than the mean giving positive or negative integers, correspondingly.

B. Ensemble Classification Methods

Followed by, the presented ILPECM-MOA method designs ensemble models such as the TCN model, SDAE method, and SLSTM technique for the classification process.

DOI: https://doi.org/10.54216/FPA.210120
Received: March 16, 2025 Revised: June 06, 2025 Accepted: July 16, 2025

1. TCN Model

TCN is one of the DL frameworks intended particularly for sequential modelling data [20]. It is proficient for the task of comprising long-term temporal dependency.

a. Sequence Modelling

Naturally, the tasks of sequential modelling. Let an input sequence $x_0, \dots, x_T$ and desire to forecast certain equivalent outputs $y_0, \dots, y_T$ at all times. The major limitation is forecasting the output y_t for a particular time t, restricted to employ those inputs that are formerly monitored: $x_0, \dots, x_t$. Afterward, a sequential modeling network contains some function $f: X^{T+1} \to Y^{T+1}$ creates the succeeding maps:

$$\hat{y}_0, \dots, \hat{y}_T = f(x_0, \dots, x_T) \quad (2)$$

Specifically, this network has been described as some function, that produces a mapping here y_t relies on $x_0, \dots, x_t$ and doesn't depend upon any upcoming input $x_{t+1}, \dots, x_T$ because of causal constraints. The objective of learning in this model's background is discovering a network f that decreases certain predictable losses among actual output and prediction indicates reducing the value of Eq. (3).

$$L\big(y_0, \dots, y_T, f(x_0, \dots, x_T)\big) \quad (3)$$

b. Causal Convolutions

To maintain the temporal order of input and impose the causal constraints, this method employs causal convolution. Within this, the output at the time became calculated utilizing only existing and previous input values, guaranteeing no upcoming data has been presented into prediction.

c. Dilated Convolutions

The modest causal convolution is simply looking back at history with linear dimensions in the network depth. It creates challenges for utilizing the abovementioned causal convolution on tasks of sequence, particularly those necessitating a long history. Solutions are applied for dilated convolutions, which allows an exponentially huge receptive area. Its major objective is increasing the receptive area of the convolutional kernel to present dilation aspects, thus acquiring longer-range temporal dependency while preserving computation efficacy.

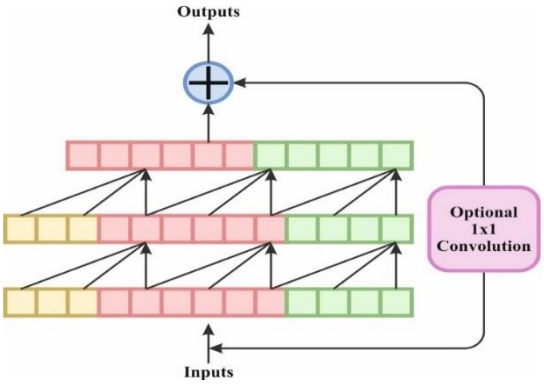

Figure 2. The Framework of the TCN Model

d. Residual Connections

Inside the TCN, residual connection is deliberated a crucial structural design focused on improving the learning features ability of the system and mitigating the possible gradient vanishing problem, which can occur in enlarged depth. The fundamental concept of residual connection is the input layer is immediately add to its output, thus offering a direct data path. The main problem of residual connection exists in handling input signals locally whereas preserving new input data. Particularly, an upstream input χ and feature representations afterward a non-linear transformation $F(x)$. To present a residual link at specified network layer, the output y is specified in Eq. (4). Within this equation y indicates the output afterward the residual link, and $F(x)$ depicts feature processed by activation function and convolutional layer. This technique permits not only learning complicated representations over non-linear transformations within the forward propagation but also preserving the reliability of input signal over the direct link. Fig. 2 specifies the framework of TCN model.

DOI: https://doi.org/10.54216/FPA.210120
Received: March 16, 2025 Revised: June 06, 2025 Accepted: July 16, 2025

$$y = F(x) + x \quad (4)$$

2. SDAE Method

SDAE surpasses at learning stronger representation of the feature by denoising input data and concentrating on important designs, making it especially suitable to identify composite and subtle attacking behaviours [21]. In comparison with traditional classifiers, SDAE uses DL to seizure nonlinear relationships and hierarchic architecture in data that increases detection precision. Its sparsity limitation guarantees computational complexity and alleviates overfitting by focusing on the important attributes. These benefits make SDAE a strong selection over traditional techniques namely RFs or SVMs for cyberattack detection in noisy dynamic environments.

AE has dual dissimilar portions, such as encoder and decoder. The encoder portion map the higher-level input data to the lower-level representations to attain sample compression and dimensionality reduction. A decoder portion transforms the lower-level abstract representations into the projected output to attain input propagation. It shows superiority in nonlinear extraction of the feature that must achieve feature vectors signifying the input database and hiding nonlinear features. The encoding and decoding methods are provided under:

$$h = f(W_1 x + \lambda_1) \quad (5)$$

During Eqs. (5) and (6), y and x represent output and input database, h represents the dimension reduction features, W_2 and W_1 refers to weights of the decoder and encoder, λ_2 and $\lambda_1$denotes output layer and the HL bias, correspondingly, and f and g specify the function of the activation.

$$y = g(W_2 x + \lambda_2) \quad (6)$$

The h size is significantly decreased in comparison with the input data, however, it even includes the input-related data. Processing and analyzing h reduces the computational overhead. Feature extraction handle nonlinear data structure. The key aim is to decrease the error of reconstruction in rebuilding the input that describes the closeness amongst the output and the input.

$$L_{AE} = \frac{1}{n}\sum_{i=1}^{n}(x_i - y_i)^2 \quad (7)$$

The AE development is accomplished by adding different limitations to L_{AE}. This method is a sparse constraint and noise coding. The sparse constraint overwhelms numerous neurons within the HL to streamline the higher-dimension data representations improve the computing cost and upgrade the speed of the system, like the NN might remove the architecture of features and samples. The noise code signifies adding noise to the input database to improve the AE performance that learns the main characteristics of the input database. Let $a^{(2)}(x^i)$ like the activation neuron's amount in h, the amount of the average activation $\wedge\, \rho \wedge \rho$ of neurons on all training instances.

$$\hat{\rho} = \frac{1}{m}\sum \begin{bmatrix} m \\ a_h^{(2)}(x^i) \\ i = 1 \end{bmatrix} \quad (8)$$

The divergence of KL has been applied to estimate the sparsity of the neurons.

$$\sum K\,L(\rho\rho) = \sum \left[\rho \log\hat{\rho} + (1-\rho)\log\frac{1-\rho}{1-\hat{\rho}}\right] \quad (9)$$

Here, ρ displays the sparsity parameter and is nearer to 0. The noise input $\wedge\, x \wedge x$ was arbitrarily formed by adding noise into the initial input x, and the output is $\wedge\, y \wedge y$. When $\wedge\, y \wedge y$ restarts x to the higher amount, it has improved efficacy.

$$L_{DAE} = \frac{1}{n}\sum_{i=1}^{n}(x_i - y_i)^2 + \frac{\lambda}{2}(\|W_1^2\|_F^2 + \|W_2^2\|_F^2) \quad (10)$$

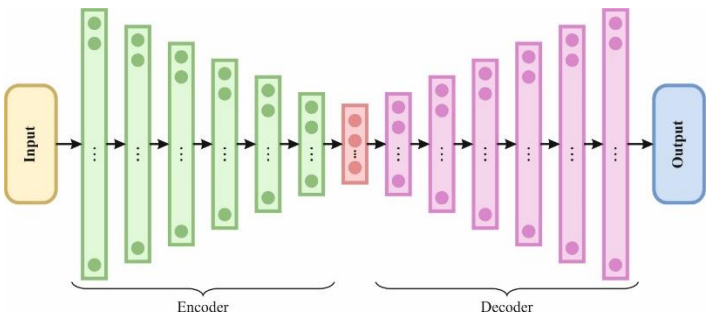

Figure 3. The Structure of SDAE Method

DOI: https://doi.org/10.54216/FPA.210120
Received: March 16, 2025 Revised: June 06, 2025 Accepted: July 16, 2025

Now, λ displays the noise-weighted limitations. The loss function LDAE of the SDAE can be provided by

$$L_{SDAE} = \frac{1}{n}\sum_{i=1}^{n}(x_i - \hat{y}_i)^2 + \beta \sum_{m=1}^{n} K\, L(\rho||\hat{\rho}) + \frac{\lambda}{2}(\|W_1^2\|_F^2 + \|W_2^2\|_F^2) \quad (11)$$

Whereas β denotes the weighted coefficient of sparsity penalty, it is made by decreasing the function of loss over the GDA. Fig. 3 indicates the structure of SDAE method.

3. SLSTM Technique

LSTM is to overwhelm the traditional RNN's drawbacks of acquiring long-term dependency owing to problem of vanishing gradient [22]. It comprises various learnable weights that work to make the output state and memory of LSTM cells. The LSTM can add or forget data to the cell's memory state utilizing gated representation. It contains 3 gates depicting forget, input, and output gates. The forget gate (f_t), stated in Eq. (12), employs the sigmoid function to existing input and hidden state to establish their contributions to upcoming state of LSTM cell. It is vital to resolve the longer-term dependency concerns. The input gate evaluates the significance of existing time-step input utilizing learnable weights on the hidden and input state representation specified in Eqs. (13,14,15). $(\hat{C}_t)$, (C_t) and (i_t) refers to present cell, updated cell states, and input gate correspondingly. In Eqs. (16,17) the output gate (O_t) employs learnable weights in hidden and input states to activation that controls the computation of cell's next hidden state (h_t) and existing output.

$$f_t = \sigma\big(W_f.[h_{t-1}, X_t] + b_f\big) \quad (12)$$

$$i_t = \sigma(W_i.[h_{t-1}, X_t] + b_i) \quad (13)$$

$$\hat{C}_t = \tanh(W_i.[h_{t-1}, X_t] + b_c) \quad (14)$$

$$C_t = f_t * C_{t-1} + i_t * \hat{C}_t \quad (15)$$

$$O_t = \sigma(W_O.[h_{t-1}, X_t] + b_o) \quad (16)$$

$$h_t = O_t * tanh(C_t) \quad (17)$$

$W_f, b_f, W_i, b_i, b_c, W_o$ and b_o refers to biased (b) and weights (W) values of respective gates, (X_t) represents input variable at time t. $(\hat{X}_t)$ indicates the output of SLSTM network at t interval. (h_{t-1}) and (C_{t-1}) refers to hidden and cell states of preceding time step $(t\text{-}1)$.

A SLSTM framework comprises many LSTM layers positioned on top of each other, here the output of single layer performs the input for next, allowing the technique for acquiring intricate hierarchical patterns in sequential data. The major advantage of employing a SLSTM is its enhanced capability for modeling complex dependency inside sequences, resulting in superior performance on challenges that require an understanding of patterns and longer-term relationships. For n^{th} layer in SLSTM: Fig. 4 represents the architecture of the SLSTM technique.

$$h_t^{(n)}, C_t^{(n)} = LSTM^{(n)}\big(h_t^{(n-1)}, h_{t-1}^{(n)}, C_{t-1}^{(n)}\big) \quad (18)$$

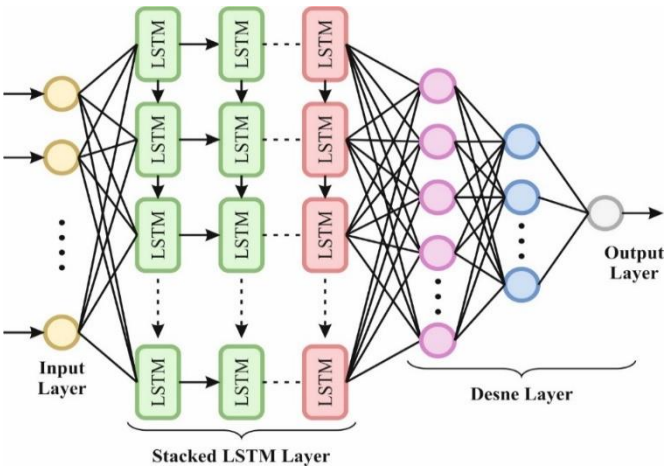

Figure 4. The Architecture of SLSTM Technique

DOI: https://doi.org/10.54216/FPA.210120
Received: March 16, 2025 Revised: June 06, 2025 Accepted: July 16, 2025

C. HEBEO-based Hyperparameter Tuning Model

At last, the HEBEO algorithm adjusts the hyperparameter values of ensemble methods and results in superior performance of classification. EOSA is a bio-inspired metaheuristic optimizer model used for various applications [23]. People in the population can shift between quarantined, hospitalized, infected, susceptible, dead, and recovered, sub-population groups because of Ebola virus's spread tactic. A new nature-inspired and population-based optimizer model is presented due to reasons for the efficiency of this tactic to spread Ebola. According to the Ebola virus's propagation mechanism, this paper offers EOSA method.

The behaviour of BESA and EOSA demonstrated that EOSA is phenomenal in outstanding global exploration courses. BESA model can guarantee a stronger local search possible. The Hybrid EOSA & BESA method is improved to discover promising solutions to the provided optimizer issue. The benefits of hybrid optimizer are captured to strengthen ability of optimization and location upgrading process and avoid dropping into local optimization problems. Now, step-wise process is described to get best classification values using HEBEO. At last, HEBEO makes uniformly distributed population to optimize best parameters. The HEBEO model is applied to support best solution.

Stage1: Initialization

Initialization of the population of EOSA & BESA model to optimize the weighted parameter generator value Ω from Dual-discriminator conditional generative adversarial networks.

$$E_i = Lower_i + rnd(0,1) \times (Upper_i + Lower_i) \qquad (19)$$

Now, $Upper_i$ and $Lower_i$ characterizes the upper and the lower limits and E_i embodies the i^{th} individual.

Stage2: Random generation

Afterward initialization, the input parameters are made at random. Now, the values of optimal fitness are chosen based on their clear hyperparameter situation.

Stage3: Approximation of Fitness Function (FF)

From initialized evaluations, the arbitrary solution was formed. The FF is evaluated with parameter optimization values to optimize weighted parameters.

$$fitnessfunction = optimization(\Omega) \qquad (20)$$

Stage4: Exploitation phase

From the perspective of statement that poor ebola will stay within zero distance or be substituted limits, the exploitation phase is generated. The individual rate of movement stated in Eq. (21),

$$E(I) = s_{rate} \times rnd(0,1) + E(Ind_{Best}) \qquad (21)$$

Now, S_{rate} characterizes the shorter distance movement.

Stage5: Exploration stage

The presumption that the ill person move out of the normal neighbourhood ranges acts as the basis for the examination stage I_{rate}. Shorter rate of movement stated in Eq. (22),

$$E(S) = l_{rate} \times rnd(0,1) + E(Ind_{Best}) \qquad (22)$$

Stage6: Selecting area for Bald Eagle

The top position for food supply of the bald eagle is chosen. New locations should be made and it is represented in Eq. (23),

$$B_n(i) = B_b(i) + \kappa.r.\left(B_m - B(i)\right) \qquad (23)$$

Now, $B_n(i)$ characterizes i^{th} newly generated location, B_b embodies gained location, B_m indicates mean location, κ signifies controller gain, and r specifies random count [0,1]. The fitness of all novel locations is projected, if some novel location provides high fitness compared to B_b, this novel location is assigned as B_b.

DOI: https://doi.org/10.54216/FPA.210120
Received: March 16, 2025 Revised: June 06, 2025 Accepted: July 16, 2025

Stage7: Searching in for Bald Eagle

The location of eagles inside the best searching region (B_b) are upgraded by model after it has been allocated. The eagle searches for prey in specified territory.

$$B_n(i) = B(i) + Y(i).B(i) - B(i+1) + x(i).(B(i) - B_m)(24)$$

Whereas, $B_n(i)$ signifies i^{th} newly made locations, $B_m$characterizes mean location, x and Y suggest directional coordinates for i^{th} location.

Stage8: Swooping Phase for Bald Eagle

The eagle shifts to discover best searching place at 3^{rd} Stage. From their most beneficial gained location, eagles travel toward their prey.

$$B_n(i) = rand.B_b + x1(i).(B(i) - \sigma 1.B_m) + Y1(i).(B(i) - \sigma 2.B_b)(25)$$

Now, $\sigma 1$ and $\sigma 2$ characterize random calculations [1,2]; $x1$ and $Y1$ signify directional co-ordinates.

Stage9: Termination Criteria

Here, the weighted parameter of generator Ω from the classification method is improved utilizing the HEBEO model, which will repeat stage 3 until the end condition.

The HEBEO model initiates a FF to acquire enhanced performance of classification. It defines an affirmative number to epitomize the superior performance of the candidate solutions.The minimization of the classification rate of error is deliberated as the FF, as provided in Eq. (26).

$$fitness(x_i) = ClassifierErrorRate(x_i)$$
$$= \frac{no\ of\ misclassified\ samples}{Total\ no\ of\ samples} * 100 \quad (26)$$

4. Evaluation Metrics and Performance Assessment

The experimental validation of ILPECM-MOA technique is inspected under Virtual Reality Experiences dataset [24]. This dataset contains 1000 total samples under five classes. The complete details of this dataset are shown below in Table 1.

Table 1: Details of dataset

Class	No. of Samples
Immersion Level-1	202
Immersion Level-2	208
Immersion Level-3	193
Immersion Level-4	206
Immersion Level-5	191
Total Samples	1000

Fig. 5 depicts the confusion matrices formed by the ILPECM-MOA method at 80:20 and 70:30 of TRPHE/TSPHE. The results denote that the ILPECM-MOA framework effectively detects and classifies all classes.

DOI: https://doi.org/10.54216/FPA.210120
Received: March 16, 2025 Revised: June 06, 2025 Accepted: July 16, 2025

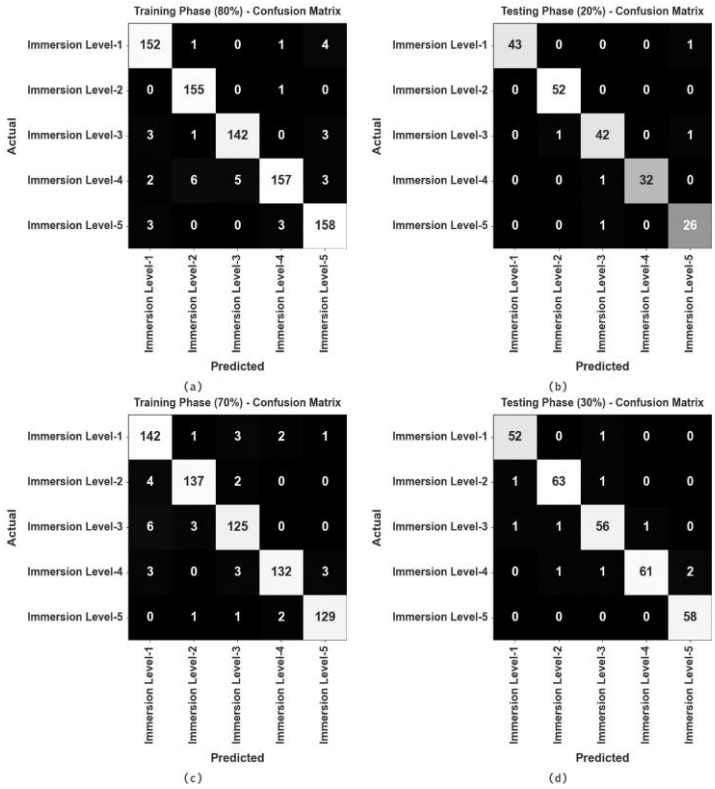

Figure 5. Confusion matrices of (a-c) TRPHE of 80% and 70% and (b-d) TSPHE of 20% and 30%

Table 2 and Fig. 6 portray the classifier result of the ILPECM-MOA framework on 80:20 of TRPHE/TSPHE. The result specified that the ILPECM-MOA technique identified all the dissimilar class labels. Under 80% TRPHE, the proposed ILPECM-MOA method obtains average $accu_y$ of 98.20%, $prec_n$ of 95.53%, $reca_l$ of 95.59%, $F_{Measure}$ of 95.53%, and MCC of 94.43%. Moreover, on 20% TSPHE, the proposed ILPECM-MOA method obtains average $accu_y$ of 99.00%, $prec_n$ of 97.28%, $reca_l$ of 97.29%, $F_{Measure}$ of 97.27%, and MCC of 96.66%.

Table 2: Classifier outcome of ILPECM-MOA model under 80:20 of TRPHE/TSPHE

Class Labels	$Accu_y$	$Prec_n$	$Reca_l$	$F_{Measure}$	MCC
TRPHE (80%)					
Immersion Level-1	98.25	95.00	96.20	95.60	94.51
Immersion Level-2	98.88	95.09	99.36	97.18	96.51
Immersion Level-3	98.50	96.60	95.30	95.95	95.03
Immersion Level-4	97.38	96.91	90.75	93.73	92.15
Immersion Level-5	98.00	94.05	96.34	95.18	93.93
Average	98.20	95.53	95.59	95.53	94.43
TSPHE (20%)					
Immersion Level-1	99.50	100.00	97.73	98.85	98.54

DOI: https://doi.org/10.54216/FPA.210120
Received: March 16, 2025 Revised: June 06, 2025 Accepted: July 16, 2025

Immersion Level-2	99.50	98.11	100.00	99.05	98.72
Immersion Level-3	98.00	95.45	95.45	95.45	94.17
Immersion Level-4	99.50	100.00	96.97	98.46	98.18
Immersion Level-5	98.50	92.86	96.30	94.55	93.70
Average	99.00	97.28	97.29	97.27	96.66

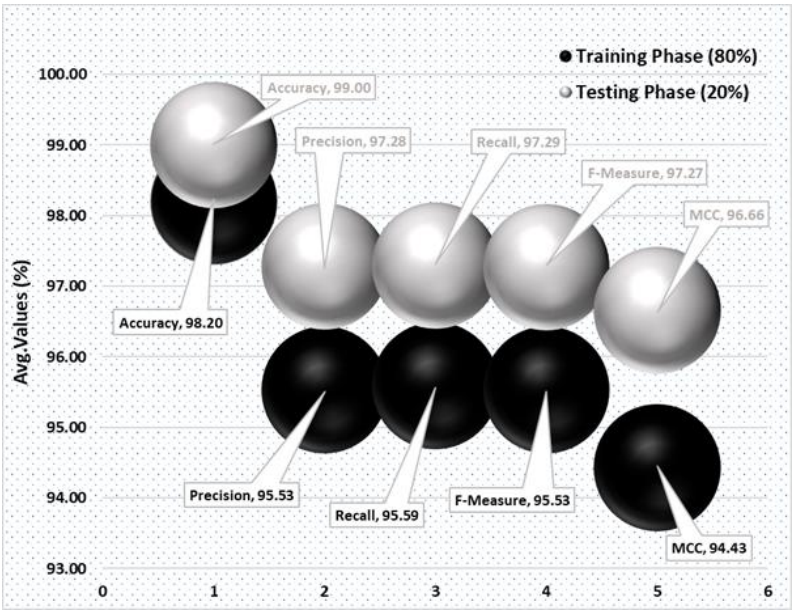

Figure 6. Average values of ILPECM-MOA model under 80%:20%

Fig. 7 demonstrates the classifier results of ILPECM-MOA approach on 80:20. Fig. 7a presents the accuracy inspection of the ILPECM-MOA framework. The figure shows that the ILPECM-MOA framework attains increasingly greater accuracy with increasing epochs. In addition, the stable rise in validation over training illustrates that the ILPECM-MOA framework excellently learns from the test dataset. Fig. 7b implies the loss examination of the ILPECM-MOA technique. The outcomes specify that the ILPECM-MOA technique accomplish closer training and validation loss values. It is indicated that the ILPECM-MOA framework learns proficiently from the test dataset.

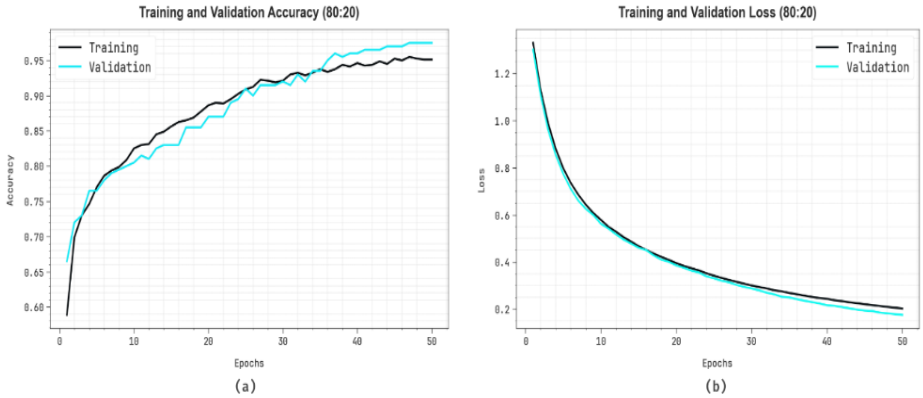

Figure 7. (a) Accuracy and (b) Loss curves under 80:20

DOI: https://doi.org/10.54216/FPA.210120
Received: March 16, 2025 Revised: June 06, 2025 Accepted: July 16, 2025

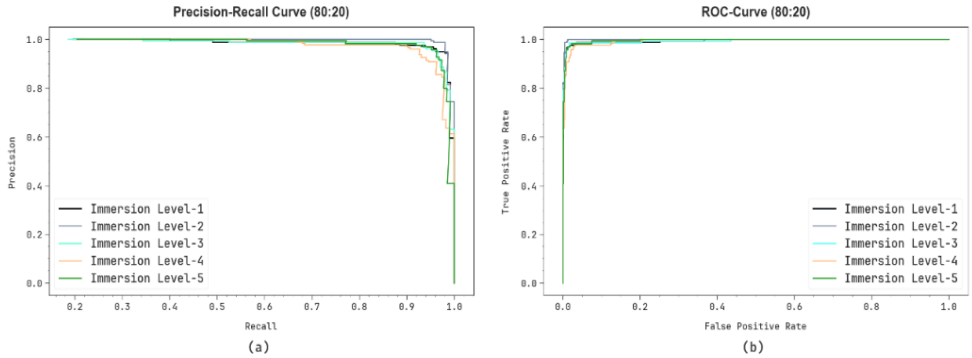

Figure 8. (a) PR and (b) ROC curves under 80:20

Fig. 8 displays the classifier results of ILPECM-MOA framework at 80:20. Fig. 8a exemplifies the PR valuation of ILPECM-MOA model. The results reported that the ILPECM-MOA model resulted in increased PR values. Furthermore, the ILPECM-MOA technique reaches supreme PR values in each class. Finally, Fig. 8b establishes the ROC inspection of the ILPECM-MOA approach. The figure elucidated that the ILPECM-MOA model attains better ROC values. Furthermore, the ILPECM-MOA model reaches superior ROC values in every class.

Table 3 and Fig. 9 represent the classifier result of ILPECM-MOA approach at 70:30 of TRPHE/TSPHE. The result defined that the ILPECM-MOA model correctly identified all the diverse class labels. Under 70% TRPHE, the proposed ILPECM-MOA model achieves average $accu_y$ of 98.00, $prec_n$ of 95.09%, $reca_l$ of 95.00%, $F_{Measure}$ of 95.03%, and MCC of 93.79%. Further, with 30% TSPHE, the proposed ILPECM-MOA technique achieves average $accu_y$ of 98.67%, $prec_n$ of 96.64%, $reca_l$ of 96.76%, $F_{Measure}$ of 96.68%, and MCC of 95.86%.

Table 3: Classifier outcome of ILPECM-MOA model under 70:30 of TRPHE/TSPHE

Class Labels	$Accu_y$	$Prec_n$	$Reca_l$	$F_{Measure}$	MCC
TRPHE (70%)					
Immersion Level-1	97.14	91.61	95.30	93.42	91.63
Immersion Level-2	98.43	96.48	95.80	96.14	95.15
Immersion Level-3	97.43	93.28	93.28	93.28	91.69
Immersion Level-4	98.14	97.06	93.62	95.31	94.17
Immersion Level-5	98.86	96.99	96.99	96.99	96.29
Average	98.00	95.09	95.00	95.03	93.79
TSPHE (30%)					
Immersion Level-1	99.00	96.30	98.11	97.20	96.59
Immersion Level-2	98.67	96.92	96.92	96.92	96.07
Immersion Level-3	98.00	94.92	94.92	94.92	93.67
Immersion Level-4	98.33	98.39	93.85	96.06	95.05
Immersion Level-5	99.33	96.67	100.00	98.31	97.91
Average	98.67	96.64	96.76	96.68	95.86

DOI: https://doi.org/10.54216/FPA.210120
Received: March 16, 2025 Revised: June 06, 2025 Accepted: July 16, 2025

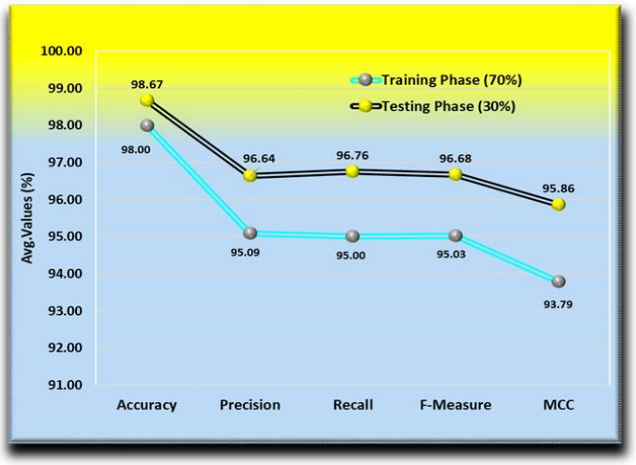

Figure 9. Average values of ILPECM-MOA model under 70%:30%

Fig. 10 displays the classifier results of ILPECM-MOA methodology at 70:30. Fig. 10a illustrates the accuracy inspection of the ILPECM-MOA model. The figure indicates that the ILPECM-MOA architecture reaches progressively higher accuracy with rising epochs. In addition, the constant progress in validation over training depicts that the ILPECM-MOA architecture efficiently learns from the test dataset. Fig. 10b exposes the loss investigation of the ILPECM-MOA model. The results signify that the ILPECM-MOA framework got similar training and validation loss values. It is emphasized that the ILPECM-MOA algorithm learns excellently from the test dataset.

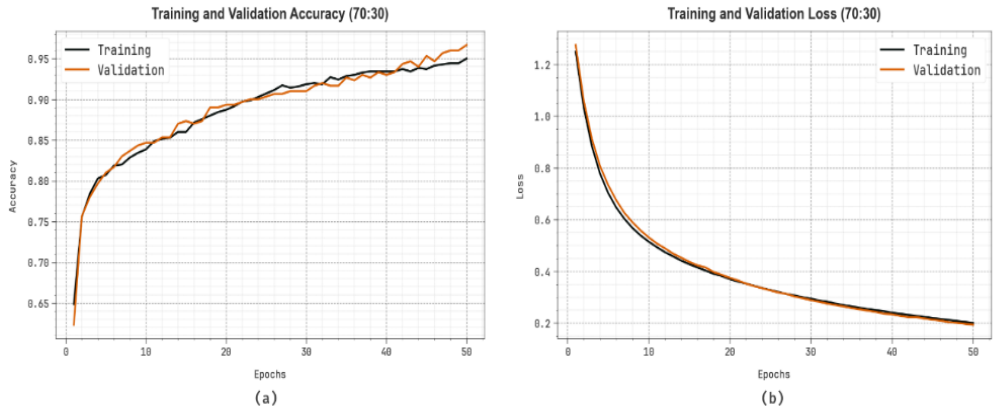

Figure 10. (a) Accuracy and (b) Loss curves under 70:30

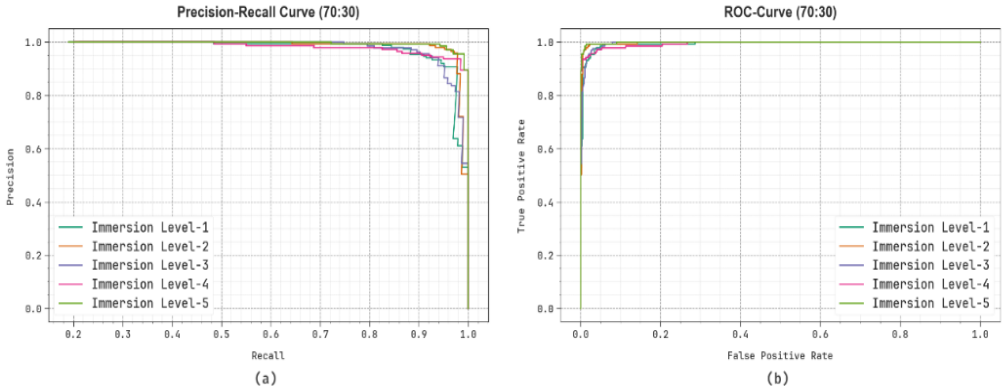

Figure 11. (a) PR and (b) ROC curves under 70:30

DOI: https://doi.org/10.54216/FPA.210120
Received: March 16, 2025 Revised: June 06, 2025 Accepted: July 16, 2025

Fig. 11 exemplifies the classifier outcomes of ILPECM-MOA system on 70:30. Fig. 11a illuminates the PR research of ILPECM-MOA method. The outcomes denoted that the ILPECM-MOA framework resulted in high PR values. Moreover, the ILPECM-MOA approach can reach maximum PR values on all class labels. At Last, Fig. 11b demonstrates the ROC analysis of the ILPECM-MOA framework. The figure illustrates that the ILPECM-MOA system provides the best ROC values. In addition, the ILPECM-MOA approach can reach better ROC values in all class labels.

Table 4 and Fig. 12 depict the comparative analysis of ILPECM-MOA model with current methodologies at several measures [25-27]. The outcomes underlined that the present models, such as kNN, SVM, RFC, MLPC, BP-MTN, LightGB, and EEGNet methodologies, have shown the worst performance compared to the proposed model. Whereas, the proposed ILPECM-MOA framework has obtained maximal $accu_y$, $prec_n$, $reca_l$, and $F_{Measure}$ of 99.00%, 97.28%, 97.29%, and 97.27%, respectively.

Table 4: Comparative analysis of ILPECM-MOA model with existing techniques

Classifiers	$Accu_y$	$Prec_n$	$Reca_l$	$F_{Measure}$
kNN Algorithm	86.05	86.06	86.07	86.07
SVM	79.06	80.07	79.06	79.05
RFC	98.85	95.82	96.42	89.93
MLPC	97.06	91.06	92.00	91.80
BP-MTN	91.05	91.06	91.07	91.05
LightGB	86.05	86.07	86.06	86.07
EEGNet	90.06	90.08	90.07	90.06
ILPECM-MOA	99.00	97.28	97.29	97.27

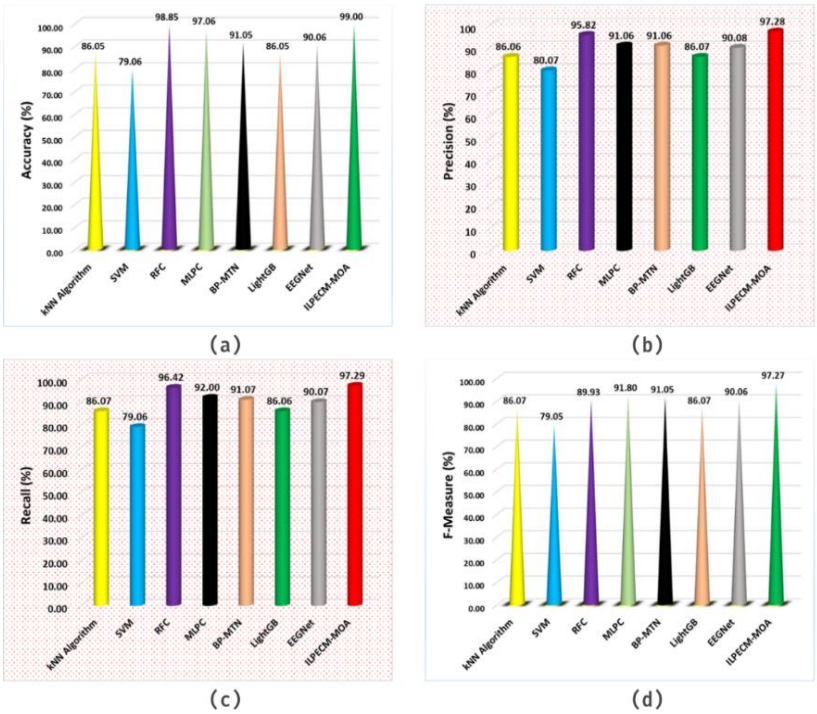

Figure 12. Comparative analysis of ILPECM-MOA model (a) $Accu_y$, (b) $Prec_n$, (c) $Reca_l$, and (d) $F_{Measure}$

DOI: https://doi.org/10.54216/FPA.210120
Received: March 16, 2025 Revised: June 06, 2025 Accepted: July 16, 2025

The processing time (PT) of ILPECM-MOA approach with the present methods is shown in Table 5 and Fig. 13. Depending on PT, the proposed ILPECM-MOA system provides a lower value of 12.79sec while the kNN, SVM, RFC, MLPC, BP-MTN, LightGB, and EEGNet approaches got higher PT of 21.21sec, 16.41sec, 24.36ec, 20.96sec, 25.89sec, 17.80sec, and 25.06sec, correspondingly.

Table 5: PT outcome of ILPECM-MOA model with recent methods

Classifiers	Processing Time (sec)
kNN Algorithm	21.21
SVM	16.41
RFC	24.36
MLPC	20.96
BP-MTN	25.89
LightGB	17.80
EEGNet	25.06
ILPECM-MOA	12.79

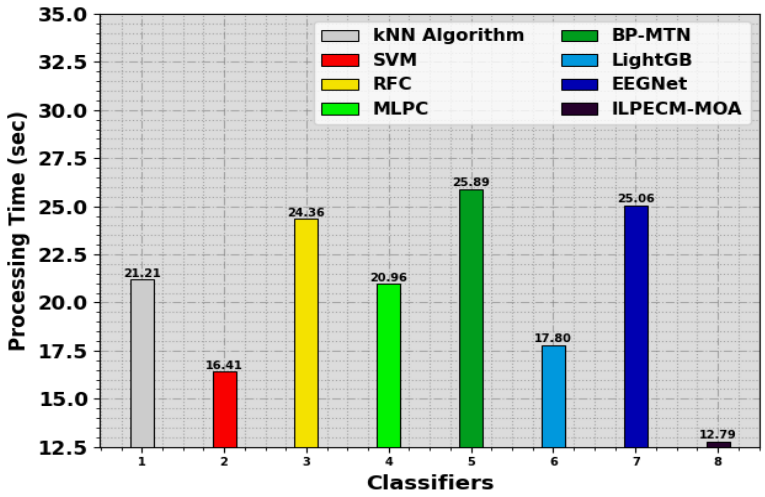

Figure 13. PT outcome of ILPECM-MOA model with recent methods

5. Conclusion

In this paper, we present an Advanced ILPECM-MOA in 3D Games Virtual Environments. This paper aims to develop a predictive model for assessing advanced immersion levels in 3D game virtual environments using behavioral and contextual data. At the primary stage, the data pre-processing stage uses Z-score normalization for transforming an input data into a beneficial pattern. Followed by, the presented ILPECM-MOA method designs ensemble models such as TCN model, SDAE method, and SLSTM technique for the classification procedure. At last, the HEBEO algorithm adjusts the hyperparameter values of ensemble methods and results in superior performance of classification. The effectiveness of the ILPECM-MOA model has been validated by the detailed studies utilizing the benchmark dataset. The mathematical outcome indicates that the ILPECM-MOA approach has improved performance and scalability in terms of various measures over the recent methods

Data Availability Statement: The data that support the findings of this study are openly available in Kaggle Dataset https://www.kaggle.com/datasets/aakashjoshi123/virtual-reality-experiences, reference number [24].

Funding: "This research received no external funding"

Conflicts of Interest: "The authors declare no conflict of interest."

DOI: https://doi.org/10.54216/FPA.210120
Received: March 16, 2025 Revised: June 06, 2025 Accepted: July 16, 2025

References

[1] F. Alam and C. Matava, "A new virtual world? The future of immersive environments in anesthesiology," *Anesthesia & Analgesia*, vol. 135, no. 2, pp. 230-238, 2022.

[2] M. Thompson, C. Uz-Bilgin, M. S. Tutwiler, M. Anteneh, J. C. Meija, A. Wang, P. Tan, R. Eberhardt, D. Roy, J. Perry, and E. Klopfer, "Immersion positively affects learning in virtual reality games compared to equally interactive 2D games," *Information and Learning Sciences*, vol. 122, no. 7/8, pp. 442-463, 2021.

[3] D. Kuťák, P. P. Vázquez, T. Isenberg, M. Krone, M. Baaden, J. Byška, B. Kozlíková, and H. Miao, "State of the art of molecular visualization in immersive virtual environments," *Computer Graphics Forum*, vol. 42, no. 6, p. e14738, Sept. 2023.

[4] J. Levy and D. Liu, "Extended Reality (XR) environments for flood risk management with 3D GIS and open source 3D graphics cross-platform game engines: advances in immersive sea level rise planning technologies for student learning and community engagement," in *International Conference on Intelligent Technologies*, Singapore: Springer Nature Singapore, pp. 271-285, Dec. 2022.

[5] S. Martirosov, M. Bureš, and T. Zítka, "Cyber sickness in low-immersive, semi-immersive, and fully immersive virtual reality," *Virtual Reality*, vol. 26, no. 1, pp. 15-32, 2022.

[6] M. C. Johnson-Glenberg, H. Bartolomea, and E. Kalina, "Platform is not destiny: Embodied learning effects comparing 2D desktop to 3D virtual reality STEM experiences," *Journal of Computer Assisted Learning*, vol. 37, no. 5, pp. 1263-1284, 2021.

[7] A. Marougkas, C. Troussas, A. Krouska, and C. Sgouropoulou, "How personalized and effective is immersive virtual reality in education? A systematic literature review for the last decade," *Multimedia Tools and Applications*, vol. 83, no. 6, pp. 18185-18233, 2024.

[8] Y. Gao, V. A. González, T. W. Yiu, G. Cabrera-Guerrero, N. Li, A. Baghouz, and A. Rahouti, "Immersive virtual reality as an empirical research tool: exploring the capability of a machine learning model for predicting construction workers' safety behaviour," *Virtual Reality*, vol. 26, no. 1, pp. 361-383, 2022.

[9] J. Taibo and J. A. Iglesias-Guitian, "Immersive 3D medical visualization in virtual reality using stereoscopic volumetric path tracing," in *2024 IEEE Conference on Virtual Reality and 3D User Interfaces (VR)*, pp. 1044-1053, Mar. 2024.

[10] H. Fares, "Catalyzing Future Education: Dynamic Learning and Remote Experiments through IoT-Integrated Learning Management Systems and Virtual Reality," *Journal of Intelligent Systems & Internet of Things*, vol. 10, no. 1, 2023.

[11] J. Lee, J. Kim, and Y. Kim, "A Head-Driven Algorithm for Estimating Upper and Lower Body Motion in Virtual Reality Environments," *IEEE Access*, 2025.

[12] M. C. Gursesli, A. Lanata, A. Guazzini, and R. Thawonmas, "Immersive virtual reality and augmented reality in human-machine interaction," in *Artificial Intelligence and Multimodal Signal Processing in Human-Machine Interaction*, pp. 331-342, Academic Press, 2025.

[13] C. Xu, Z. Chen, M. Tao, and W. Zhang, "Wireless Multi-User Interactive Virtual Reality in Metaverse with Edge-Device Collaborative Computing," *IEEE Transactions on Wireless Communications*, 2025.

[14] B. Lyu and Y. Wang, "Immersive visualization of 3D subsurface ground model developed from sparse boreholes using virtual reality (VR)," *Underground Space*, vol. 17, pp. 188-206, 2024.

[15] A. Ojha, S. Narain, A. Raj, T. Agrawal, B. Wadhwa, and M. Joshi, "Dynamic virtual reality horror sports enhanced by artificial intelligence and player modeling," *Multimedia Tools and Applications*, vol. 83, no. 32, pp. 77415-77432, 2024.

[16] A. Kumar, A. K. J. Saudagar, M. Alkhathami, B. Alsamani, M. B. Khan, M. H. A. Hasanat, Z. H. Ahmed, A. Kumar, and B. Srinivasan, "Gamified learning and assessment using ARCS with next-generation AIoMT integrated 3D animation and virtual reality simulation," *Electronics*, vol. 12, no. 4, p. 835, 2023.

[17] Y. Yamazaki and S. Hasegawa, "Providing 3D guidance and improving the music-listening experience in virtual reality shooting games using musical vibrotactile feedback," in *2023 IEEE Conference on Virtual Reality and 3D User Interfaces (VR)*, pp. 276-285, Mar. 2023.

DOI: https://doi.org/10.54216/FPA.210120
Received: March 16, 2025 Revised: June 06, 2025 Accepted: July 16, 2025

[18] J. Agarwal and S. Shridevi, "Procedural content generation using reinforcement learning for disaster evacuation training in a virtual 3D environment," *IEEE Access*, vol. 11, pp. 98607-98617, 2023.

[19] R. Munshi and S. K. G. Gupta, "Innovative Diagnostic Strategies for Identifying High-Risk Patients Using Laboratory Parameters," *SGS-Engineering & Sciences*, vol. 1, no. 1, 2025.

[20] W. Li, Y. Guo, S. Li, Y. Gao, and Y. Qu, "Inversion Method Based on Temporal Convolutional Networks for Random Ice Load on Conical Offshore Platforms," *Journal of Marine Science and Engineering*, vol. 13, no. 5, p. 1000, 2025.

[21] E. Yang, S. Jeong, and C. Seo, "Harnessing feature pruning with optimal deep learning based DDoS cyberattack detection on IoT environment," *Scientific Reports*, vol. 15, no. 1, pp. 1-15, 2025.

[22] S. R. Vangipuram and A. V. Giridhar, "Short Term Residential Load Forecasting Using Temporal Weather Based Embedding Stacked LSTMs," *IEEE Latin America Transactions*, vol. 23, no. 6, pp. 497-507, 2025.

[23] P. Yenuga, S. N. R. Beeram, S. S. Parvathi, G. M. Reddy, V. Boppana, S. Davuluri, R. Ramesh, M. Srikanth, B. V. P. Rao, R. K. Munaganuri, and N. Rao, "Optimized Self-Attention Pyramidal Convolutional Neural Network for Intrusion Detection Framework in IoT," *Journal of Advances in Information Technology*, vol. 16, no. 5, 2025.

[24] "Virtual Reality Experiences Dataset," *Kaggle*, [Online]. Available: https://www.kaggle.com/datasets/aakashjoshi123/virtual-reality-experiences.

[25] M. S. Anwar, J. Wang, W. Khan, A. Ullah, S. Ahmad, and Z. Fei, "Subjective QoE of 360-degree virtual reality videos and machine learning predictions," *IEEE Access*, vol. 8, pp. 148084-148099, 2020.

[26] C. E. Orozco-Mora, D. Oceguera-Cuevas, R. Q. Fuentes-Aguilar, and G. Hernández-Melgarejo, "Stress level estimation based on physiological signals for virtual reality applications," *IEEE Access*, vol. 10, pp. 68755-68767, 2022.

[27] Z. Wang, Y. Yan, J. Cai, C. Hua, N. Liu, Q. Chen, M. Li, and D. Zhang, "VR vertigo level classification using a multi-dimensional Taylor network approach," *IEEE Access*, vol. 11, pp. 108944-108955, 2023.

DOI: https://doi.org/10.54216/FPA.210120
Received: March 16, 2025 Revised: June 06, 2025 Accepted: July 16, 2025